Acta Chemica Scandinavica, 1997: 51: 455–461
Printed in UK – all rights reserved

ACTA
CHEMICA SCANDINAVICA
ISSN 0904–213X

The $CsBr–AlBr_3$ Phase Diagram and the Crystal Structure of $CsAlBr_4$

Rolf Willestofte Berg

Department of Chemistry, DTU 207, The Technical University of Denmark, Building 207, DK-2800 Lyngby, Denmark

Berg, R. W., 1997. The $CsBr–AlBr_3$ Phase Diagram and the Crystal Structure of $CsAlBr_4$. – Acta Chem. Scand. 51: 455–461. © Acta Chemica Scandinavica 1997.

The phase diagram in the $CsBr–AlBr_3$ system has been reinvestigated. An adjusted liquidus diagram is given, showing the compound $CsAlBr_4$, which melts congruently at 360 °C. The lack of consistency among previous results is presumably due to the presence of oxide impurities formed by attack of bromide on the silica ampule walls. Some molten salt density data are given. The $CsAlBr_4$ crystal structure has been solved in the orthorhombic space group *Pnma*, no. 62 (D_{2h}^{16}), with $a=12.2137(20)$, $b=7.5304(14)$ and $c=9.9293(16)$ Å, by means of X-ray powder diffraction and full-profile Rietveld refinements, converging with $R_P=0.0952$ and $R_{WP}=0.1236$ ($R_{expected}=0.0509$, 'goodness of fit' = 2.42, Bragg R-factor = 0.0419, and derived $R_F=0.0458$). The $AlBr_4$ tetrahedron is almost regular, with Al–Br bond distances in the range 2.20–2.35 Å, in accordance with what is to be expected from previous related structure determinations.

CsBr and $AlBr_3$ (or rather Al_2Br_6) are well known solid compounds. However, the binary $CsCl–AlBr_3$ temperature–composition phase system has been little investigated.[1–3] It appears that two independent examinations were published in the years 1967–68[1,2] and that one, from 1977, was in fact a quotation.[3] The results of these works were not particularly consistent; e.g. Cronenberg *et al.*[1] found the melting point of $CsAlBr_4$ to be 357 °C, whereas Mikheeva *et al.*[2] reported a value of 340 °C. Also, in other details their results differed appreciably. Therefore, it was decided to determine the melting points of some selected compositions to improve the knowledge of this phase diagram. The congruently melting 1:1 compound, $CsAlBr_4$, is known to form crystals of orthorhombic symmetry, with $a=12.18(3)$, $b=7.50(2)$ and $c=9.89(2)$ Å, and with four molecules per unit cell.[4] The crystals were said to be isomorphous with $BaSO_4$ and $CsGaBr_4$, in space group *Pnma*, no. 62. The crystal structure was not solved, so the parameters were determined during this work. A redetermination of the crystal structure of Al_2Br_6 is reported elsewhere.[5]

Experimental

Owing to the extreme moisture sensitivity of aluminium bromide compounds, all operations were carried out in a drybox, and chemicals were stored in vacuum-sealed ampules. $AlBr_3$ was made by letting bromine react dropwise with pure aluminium metal in a vessel (carefully cooled with a reflux column). The crude $AlBr_3$ formed was purified by distillation over more aluminium and further purified by three subsequent recrystallizations under vacuum in sealed ampules, decanting 30% each time. CsBr (Merck AG, suprapur) was used after drying under vacuum for several days at 200 °C. For the melting-point experiments, pre-weighed quantities were put into quartz cells which were sealed under vacuum, outside the box. The cells were equipped with a thermometer pocket at the bottom, allowing for melting-point determination in a carefully controlled furnace, by use of a calibrated 100 Ω Pt resistance thermometer. The equilibrium melting point was established after repeated recording of temperature and opening of the furnace for visual inspection. The purity of the pre-equilibrated samples was investigated by means of Raman spectroscopy; a small content of oxide was invariably found.[6] Other experimental details are given elsewhere, see e.g. Refs. 5–7. For X-ray data collection, powdered $CsAlBr_4$ containing a small excess of CsBr was placed inside a home-made moisture-protective container for use under Bragg–Brentano scattering geometry, with a sampling area of ca. 1 cm^2, and with a window of thin polyethylene/aluminium/polyethylene laminated foil.[5] Diffractograms were obtained with a Philips PW1820/PW3711 automated $\theta/2\theta$ powder diffractometer using Cu$K\alpha$ radiation ($\lambda_1=1.5406$ Å, $\lambda_2=1.5444$ Å, intensity ratio = 0.5), a variable slit-width, a 2θ step size of 0.02°, a counting time of 5 s per step, and a temperature of 25 °C.

Results and discussion

Phase diagram. The new melting points in the $CsBr–AlBr_3$ phase diagram are summarized in Table 1. The

Table 1. Observed solidus and liquidus points in the CsBr–$AlBr_3$ phase diagram and density data, in dependence of mole fractions X, calculated from weights.

X($AlBr_3$)	X(CsBr)	T_s/°C solidus	T_0/°C liquidus	Density at melting point/g cm^{-3}
1.0	0.0	–	97	<2.65[a]
0.74883	0.25117	135	142	ca. 2.67[b]
0.67016	0.32984	150	211	
0.5[c]	0.5	359	360	
0.49936	0.50064	335	344	
0.47776	0.52224	–	340	ca. 3.16[b]
0.45660	0.54340	–	333	
0.46163	0.53837	–	336	
0.43141	0.56859	330	402	ca. 3.10[b]
0.35046	0.64954	–	501	ca. 3.48[b]
0.00000	1.00000	–	636	ca. 4.02[d]

[a] According to Olson et al.[13]. [b] Estimated in this work. [c] $CsAlBr_4$ refined by repeated recrystallization. Mole fractions given, assuming purity. [d] According to extrapolation.[8,9]

total amount of data known from this work and previous studies[1–3] are depicted in Fig. 1. In the temperature range studied here, CsBr adopts only one phase, the cubic CsCl-type modification crystallizing[8] in space group $Pm\bar{3}m$, no. 221, $Z=1$, with a lattice constant of 4.2953 Å and a calculated density of 4.455 g cm^{-3} at 25±1 °C. From the known thermal expansion,[9] the density of crystalline CsBr can be calculated, e.g. at 625 °C, to about 4.02 g cm^{-3}. At low temperature, below ca. −115 °C, CsBr can adopt the rock-salt structure, space group $Fm\bar{3}m$, no. 225, $Z=4$, and with a lattice constant of 7.253 Å, at −118 °C.[10] The melting point, T_0, of CsBr is 636 °C or 909 K.[11,12] From T_0 and the known[11] heat of fusion ($\Delta H_{fus}=5640$ cal $mol^{-1}=23606$ J mol^{-1}), the limiting slope of the CsBr liquidus branch can be found using the Raoult–van't Hoff relation [eqn. (1)]

$$-R \ln X=\Delta H_{fus}(1/T-1/T_0)=\Delta H_{fus}(T_0-T)/(T\,T_0) \quad (1)$$

X is the mole fraction of CsBr and T the absolute temperature on the liquidus branch (at $X=1$, $T=T_0$). Near $X=1$, the first term approximation $\ln X\approx(X-1)=X(AlBr_3)$ is quite valid. Hence, the limiting slope at $X=1$, $dT/dX(AlBr_3)$, is equal to $RT_0^2/\Delta H_{fus}$. The slope calculates to −291 K per unit of mole fraction X and is included in Fig. 1. At the other end of the diagram, the melting point and the critical temperature of $AlBr_3$ is 97.5 and 490 °C, respectively, according to available literature data.[13] Aluminium bromide is dimeric in the solid as well as in the liquid and gaseous states at moderate temperatures.[5]

Density. It was observed during this work that the density of a basic melt ($AlBr_3$ mole fraction equal to ca. 0.43) was around 3.10 g cm^{-3} at the melting point (near 402 °C). In another experiment, a piece of pure aluminium metal (having nominally a density of 2.698 g cm^{-3} at 20 °C and a coefficient of linear thermal expansion of 23.03×10^{-6} K^{-1}) was able to float on the surface of the acidic eutectic CsBr–$AlBr_3$ melt ($AlBr_3$ mole fraction equal to 0.67) at ca. 150 °C, but sank to the bottom at ca. 220 °C. This indicates that the density of such a melt becomes equal to that of aluminum, i.e. ca. 2.67 g cm^{-3}, at a temperature in the neighborhood of 185 °C. Also in an experiment in the two-liquid region, aluminium was found, at ca. 250 °C, to be more dense than both the upper $AlBr_3$ phase and the lower CsBr–$AlBr_3$ phase in contact herewith, whereas at ca. 200 °C the aluminium piece was able to float on the surface between the upper and the lower liquid phases. This indicates that the

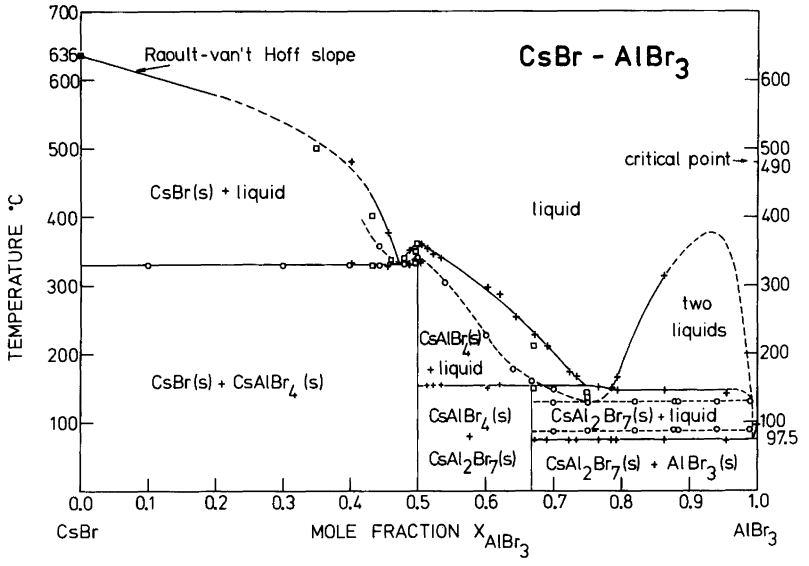

Fig. 1. Phase diagram of the CsBr–$AlBr_3$ system, according to all available information. (+) Cronenberg *et al.*[1] (○) Mikheeva *et al.*[2] (■) Dworkin *et al.*[11] (□) This work.

density of the denser phase, in the demixing range of the phase diagram, is around 2.67 g cm^{-3} at about 225 °C. The density of liquid $AlBr_3$ is precisely known as a function of temperature, and is less than 2.65 g cm^{-3} at all temperatures.[13]

Reactivity with glass. The stability of silica ampule walls towards bromide–oxide exchange corrosion was examined by testing for the presence of any condensable $SiBr_4$ gas in the vacuum-sealed cells before and after they have been equilibrated in the furnace. On cooling the unopened 'spent' cells locally by means of liquid nitrogen, a clearly observable amount of colorless gas could be condensed as a liquid which later became solid. No condensable gas was seen before the first melting of the reagents.

Discussion. The melting points observed by us generally fall between high values of Cronenberg *et al.*[1] and low values of Mikheeva *et al.*[2] (Fig. 1). It is likely that the results of Cronenberg *et al.*[1] are slightly too high due to their use of a rather fast heating rate (0.5 °C min^{-1}) in a liquid bath. The results of Mikheeva *et al.*[2] might be less accurate, possibly due to impurities in their chemicals or corrosion of the silica walls, as discussed below.

The melting points observed during the present work proved to be unstable, decreasing with time. Obviously, a corrosion reaction occurred between the melt and the silica container material, especially in the basic range (more CsBr than $AlBr_3$), perhaps enhanced by the high temperature. The corrosion seems to be similar to the one seen during our study[7] of the $CsCl–AlCl_3$ phase system. By analogy, we assume the following corrosion reactions to occur in the acidic [eqn. (2)] or basic [eqn. (3)] ranges of the phase diagram (n and m are unknown):

$$2AlBr_3 + SiO_2(s) \rightarrow 2/n(AlOBr)_n + SiBr_4 \quad (2)$$

$$4CsBr + 2SiO_2(s) \rightarrow 1/m(Cs_4SiO_4)_m + SiBr_4 \quad (3)$$

In both cases colorless $SiBr_4$ gas should be formed. This is in accord with the observed presence of traces of a condensable gas after melting. By means of Raman spectroscopy, we looked after traces of $SiBr_4$ in some of the cells after melting. $SiBr_4$ (prepared from silicon and bromine in this laboratory) had Raman bands near 90, 135 and 246 cm^{-1} as a liquid at 25 °C; and near 85, 133 and 246 cm^{-1} as a gas at 125 °C. The strong 246 cm^{-1} band (the totally symmetric Si–Br stretching) was seen in most of the heated cells, indicating that the reactions

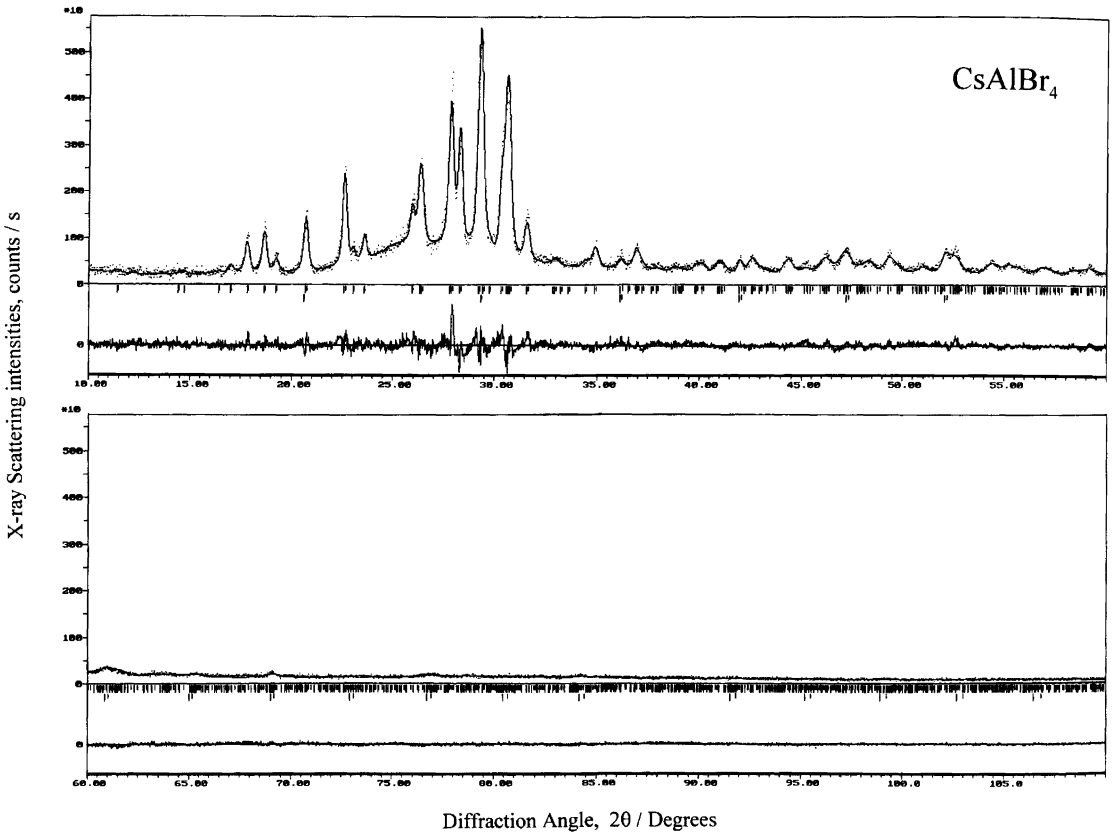

Fig. 2. X-Ray powder diffractogram of $CsAlBr_4$ (points) in 2θ ranges 10–60° and 60–110°. The solid line is the best-fit Rietveld profile. Tick marks below the profile indicate positions of all allowed copper $K\alpha_1$ (long) and $K\alpha_2$ (short) Bragg peaks, the lower set representing the CsBr minority phase. The difference between the observed and calculated intensities is shown in the bottom fields.

[eqns. (2) and (3)] definitely have taken place to some extent.

A consequence of reactions [eqns. (2) and (3)] should be a progressive formation of oxide or silicate species depressing the melting point, as discussed previously.[14] Therefore, it is not surprising that unstable melting points were obtained, decreasing with time. The large scatter in the results obtained by the various researchers (Fig. 1) can, at least in part, be explained as being due to bromide–oxide exchange reactions on the silica surfaces. This might be the reason for Cronenberg *et al.*[1] to adopt their fast heating rate.

Structure of $CsAlBr_4$. Figure 2 shows the obtained X-ray diffraction pattern of the $CsAlBr_4$ powder. Prior to the data analysis, five different recordings were averaged in order to minimize sampling errors (height and preferred orientation of crystallites). The pattern was then indexed by using 20 *d*-values of well resolved lines as input data to the TREOR and PIRUM programs of Werner.[15,16] The only result was an orthorhombic unit cell with axes 12.202(5), 7.558(9) and 9.932(5) Å. All 20 lines were indexed. The 'M_{20} figure-of-merit' of de Wolf[17] and the 'F_{20} criterion' of Smith and Snyder[18] were both calculated as ca. 7 after refinement with the PIRUM program. The $CsAlBr_4$ diffractogram was thus considered as essentially solved. The systematic extinctions were in accordance with the space group *Pnma* found by Gearhart *et al.*[4] (based on single-crystal Weissenberg film work), but our unit-cell volume was slightly larger (Table 2). Then, the intensity data were corrected for variation in slit-width and subjected to Rietveld full-profile refinements,[19] using the PC program of Young and coworkers.[20–22] Atomic scattering amplitudes and a monochromator polarization correction factor of 0.85 were used. The background was represented by linear interpolation between 24 data points, selected between the peaks in the pattern. The program uses a Newton–Raphson least-squares minimization algorithm and a weighting scheme of $w_i = 1/y_{i,\mathrm{obs}}$, where $y_{i,\mathrm{obs}}$ represents the observed intensity at the *i*th step (after slit-width and Lorentz-polarisation corrections). The refinements included scaling factors for each phase ($CsAlBr_4$ + very little of CsBr), zero shift, pseudo-Voigt Bragg peak-profile parameters, and lattice, positional and thermal parameters. The refinements were conducted stepwise involving more and more free parameters until shifts were <5% of their associated e.s.d.s. Peaks below $2\theta = 30°$ were corrected for asymmetry. Surface roughness and preferred orientation were of minor importance. No correction was done for absorp-

Table 2. Crystal data (25 °C) and Rietveld profile parameters for $CsAlBr_4$ and, for comparison $CsGaBr_4$, in orthorhombic space group Pnma (no. 62, D_{2h},[16] $Z = 4$).[a]

Formula	$CsAlBr_4$	$CsAlBr_4$	$CsGaBr_4$
	This work	Ref. 4	Ref. 4
Formula weight/g mol^{-1}	479.52	479.52	522.26
V/Å^3	913.24	903.45	897.91
a/Å	12.2137(20)	12.18(3)	12.15(3)
b/Å	7.5304(14)	7.50(2)	7.48(2)
c/Å	9.9293(16)	9.89(2)	9.88(2)
D_{calcd}/g cm^{-3}	3.49		3.86
Profile range ($2\theta_{\mathrm{max}}$/°)	10–110		
No. of observations, N	5000		131 observed and 66 absent of 345 possible
No. of independent contributing reflections	1250 (+42 from CsBr)		
No. of parameters, P	35		
Peak range (in units of H_K)[b]	7		
Pseudo-Voigt profile shape Lorentzian fraction, η[c]	0.634		
Half-width parameters, U and U_{CsBr}[d]	4.99(24), 3.04(23)		
Half-width parameters, V and V_{CsBr}[d]	−2.12(12), −1.76(11)		
Half-width parameter, W	0.284(15)		
CsBr lattice parameter, a/Å[d]	4.3009(7)[e]		
Asymmetry parameter,[f] for $CsAlBr_4$ peaks below $2\theta = 30°$	0.54(3)		
$R_P = \Sigma\lvert y_{\mathrm{obs},i} - y_{\mathrm{calc},i}\rvert / \Sigma y_{\mathrm{obs},i}$	0.0952		
$R_{wp} = [\Sigma w_i (y_{\mathrm{obs},i} - y_{\mathrm{calc},i})^2 / \Sigma w_i (y_{\mathrm{obs},i})^2]^{\frac{1}{2}}$	0.1236		
$R_{\mathrm{expected}} = [(N-P)/\Sigma w_i y_{\mathrm{obs},i}^2]^{\frac{1}{2}}$	0.0509		
'Goodness of fit', $S = R_{wp}/R_{\mathrm{expected}}$	2.42		
Bragg peak intensity R-factor $= \Sigma\lvert I_{\mathrm{obs,K}} - I_{\mathrm{calc,K}}\rvert / \Sigma I_{\mathrm{obs,K}}$	0.0419		
Derived structure amplitude $R_F = \Sigma\lvert\lvert F_{\mathrm{obs,K}}\rvert - \lvert F_{\mathrm{calc,K}}\rvert\rvert / \Sigma\lvert F_{\mathrm{obs,K}}\rvert$	0.0458		$R_{\mathrm{final}} = 0.21$[g]

[a] Estimated standard deviations on last digits are given in parentheses. [b] H_K is the full width at half maximum of the *K*th Bragg reflection. The angular dependence is represented by the expression $H_K^2 = U\tan^2\theta + V\tan\theta + W$. [c] The profile function was a sum of a Lorentzian part, ηL, and a Gaussian part, $(1-\eta)G$, as defined by Young *et al.*,[20–22] applied without angle dependence. [d] A small amount of CsBr was present in the sample. The *B*-values of Cs and Br in CsBr were 2.51(52) and 4.25(81) Å^2. [e] A value of 4.2953 Å is given in the literature.[8] [f] Peak asymmetry parameter as defined by Rietveld.[19] [g] Based on Mo*K*α Weissenberg film intensities read with a densitometer and corrected for absorption.[4]

tion effects. (Such corrections are normally not necessary for Bragg–Brentano geometry.[21]) Refinement of site occupancies did not show significant deviations from stoichiometry. In the refinements, the thermal parameter of Br1 was large unless refined anisotropically.

The final lattice constants of $CsAlBr_4$ and details of data collection and profile analysis are shown in Table 2. Positional parameters and temperature factors are listed in Table 3 and the unit cell is depicted in Fig. 3. The observed and calculated peak intensities for 19 selected strong peaks are listed in Table 4. The final calculated profile is included in Fig. 2. Interatomic distances and angles of the $AlBr_4$ tetrahedron are given in Table 5.

Discussion Comparison of our structure refinement results on $CsAlBr_4$ with those of Gearhart *et al.*[4] on $CsGaBr_4$ (single crystal film-work) demonstrates that the gallium and aluminium-containing crystals are indeed isomorphous (isostructural) and have very similar parameters (cf. Tables 2 and 3). Both crystals certainly belong to the $BaSO_4$ type. This is also in accord with the systematics of Staffel and Meyer,[23] who also have found $RbAlBr_4$ to belong to the $BaSO_4$ type.

Table 5 shows that the found $AlBr_4$ tetrahedron has an almost regular cubic symmetry; the Br–Al–Br bond angles being close to the regular tetrahedral angle of 109.47°. The Al–Br bond lengths are close to 2.3 Å. The values found can be compared with previously reported $AlBr_4$ tetrahedra as shown in Fig. 4, which is based on other solved related crystal structures.[5,24–27] Our new data fit nicely into the picture, as can be seen. The Al–Br bond lengths found are also near the value of 2.35 Å which can be calculated, summing the ionic radii of six-coordinated Br^- (1.96 Å) and four-coordinated Al^{3+} (0.39 Å).[28] The *R*-values (Table 3) are not as low as one would wish.

The standard deviations obtained are considered to be underestimated. (They should probably be multiplied by 2 or 3 to give realistic values.) The isotropic thermal parameters (*B*-values) are larger than the 1–2 $Å^2$ expected. The reason is probably that the *B*-values cover some deficiencies in the model.

Table 3. Fractional coordinates and equivalent isotropic thermal parameters for the atoms in $CsAlBr_4$. For comparison, coordinates of $CsGaBr_4$ due to Gearhart *et al.*,[4] are given in italics.[a]

Atom	*x/a*		*y/b*		*z/c*		$B^b/Å^2$
Cs	0.1758(4)	*0.1810(10)*	0.25		0.1763(6)	*0.173(4)*	3.44(16)
Al	0.0663(20)	*0.0677(30)*	0.25		0.6927(24)	*0.692(11)*	2.18(68)
Br1	−0.0890(12)	*−0.0925(20)*	0.25		0.5800(9)	*0.575(6)*	ca. 2.31[c]
Br2	0.2191(9)	*0.215(20)*	0.25		0.5493(8)	*0.555(7)*	4.37(32)
Br3	0.0808(4)	*0.0825(9)*	0.0097(7)	*0.0054(13)*	0.8315(5)	*0.825(3)*	2.05(12)

[a] Atoms on Wyckoff sites *c*(*x*, 1/4, *z*) are of multiplicity 4 and have a mirror site symmetry (the *y*-coordinates are fixed by symmetry). Br3 on general Wyckoff site *d* is of eight-fold multiplicity and with no site symmetry. The estimated standard deviation of the last digit is given in parantheses. [b] *B* is the isotropic temperature factor as defined by Young *et al.*[20–22] [c] The anisotropic *B*-matrix diagonal elements found were $B(1,1)=0.01\pm0.76$, $B(2,2)=0.08\pm2.02$ and $B(3,3)=0.02\pm1.16$. Off-diagonal elements were zero.

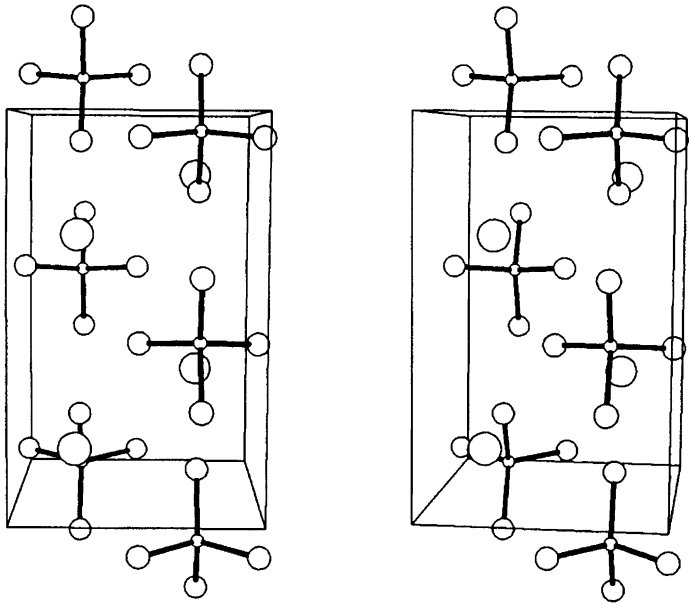

Fig. 3. Stereo-plot of the unit cell of $CsAlBr_4$, seen along the *c*-axis. The *a*-axis is vertical and the *b*-axis is horizontal.

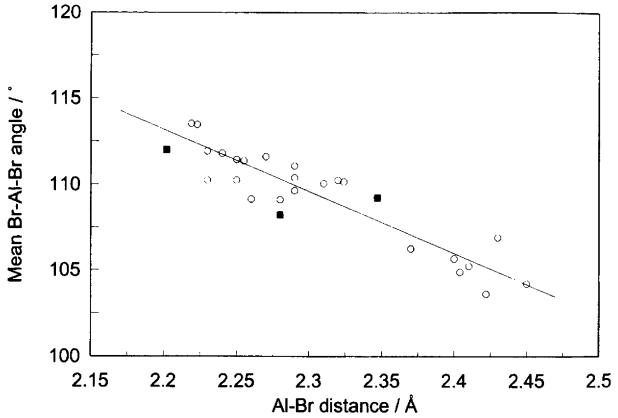

Fig. 4. Plot of the found average of the three Br–Al–Br angles involving a particular Al–Br bond versus that Al–Br bond distance (four filled squares, one on top of another). Also shown (as circles) are 24 points calculated from data in the literature.[5,24–27] The line is a regression line of all points.

Table 4. Calculated and observed Cu$K\alpha_1$ intensities for selected strong reflections of $CsAlBr_4$, as a function of Miller indices and 2θ values.

h	*k*	*l*	2θ/°	I_{calcd}[a]	I_{obsd}[a]
0	0	2	17.803	8460	8589
2	1	0	18.645	11444	11824
2	1	1	20.693	13376	13424
1	1	2	22.595	22992	24663
0	2	0	23.571	5944	6416
2	1	2	25.923	9407	12000
1	2	1	26.289	12059	12228
3	1	1	26.400	11547	11575
2	2	0	27.780	14091	14746
1	0	3	27.873	25707	27376
3	0	2	28.294	30642	28251
2	2	1	29.226	30434	30834
1	1	3	30.340	18647	20302
4	0	1	30.578	19466	19402
1	2	2	30.633	22285	22072
3	0	3	34.885	6594	6123
3	2	3	42.564	6100	5921
3	2	4	49.294	9098	9325
5	2	3	52.475	7970	8697

[a] Exclusive background and un-normalized.

Table 5. Bond and contact lengths (in Å), and angles (in °) for $CsAlBr_4$.[a]

Bond lengths/Å		Bond angles/°	
Al–Br1	2.02(2)	Br1–Al–Br2	112.1(3)
Al–Br2	2.35(2)	Br1–Al–Br3 (×2)	111.9(3)
Al–Br3	2.28(2) (×2)	Br2–Al–Br3 (×2)	107.7(3)
		Br3–Al–Br3	105.0(3)
Nonbonded contacts/Å			
Cs–Br1	3.83(2)[b]	Br1–Br2	3.75(5)
Cs–Br2	3.74(2)[b]	Br1–Br3	3.76(5)
Cs–Br3	3.88(2)[b]	Br2–Br3	3.72(5)
Cs–Cs	6.49(2), 6.70(2)	Br3–Br3	3.62(5)

[a] Estimated standard deviations are not precise. [b] In CsBr crystals, the contact distance has been found[8] to be 3.713 Å.

Acknowledgements. I acknowledge the use of X-ray powder pattern indexing programs TREOR90 and PIRUM by P.-E. Werner of University of Stockholm, Sweden, and of the Rietveld refinement program DBWS-9411 by R.A. Young and co-workers of Georgia Institute of Technology, Atlanta, Georgia, USA. The advice and help of T. Østvold, University of Trondheim, Norway, of G.N. Papatheodorou, University of Patras, Greece, of Bernard P. Gilbert, University of Liège, Belgium and Kurt Nielsen of this university are appreciated. The Danish Technical Research Council supported the project.

References

1. Cronenberg, C. T. H. M. and van Spronsen, J. W. *Z. Anorg. Allgem. Chem. 354* (1967) 103.
2. Mikheeva, V. I., Arkhipov, S. M. and Revzina, T. V. *Russ. J. Inorg. Chem. 13* (1968) 884.
3. Mascherpa-Corral, D. and Potier, A. *J. Chim. Phys. (Paris) 74*(1977) 1077.
4. Gearhart Jr., R. C., Beck, J. D. and Wood, R. H. *Inorg. Chem. 14* (1975) 2413.
5. Berg, R. W., Nielsen, K. and Poulsen, F. W. *Acta Chem. Scand. In Press.*
6. Gilbert, B. P., Berg, R. W. and Bjerrum, N. J. *Appl. Spectrosc. 43* (1989) 336.
7. Berg, R. W., Lauridsen, T. L., Østvold, T., Hjuler, H. A., von Barner, J. H. and Bjerrum, N. J. *Acta Chem. Scand., Ser. A 40* (1986) 646.
8. Swanson, H. E., Fuyat, R. K. and Urinic, G. M. *Natl. Bur. Stand. USA Circ. 539, III* (1954) 49.
9. Johnson, J. W., Agron, P. A. and Bredig, M. A. *J. Am. Chem. Soc. 77* (1955) 2734.
10. Blackman, M. and Khan, I. H. *Proc. Phys. Soc. (London) 77* (1961) 471.
11. Dworkin, A. S. and Bredig, M. A. *J. Phys. Chem. 64* (1960) 269.
12. Plyushchev, V. E. and Samuseva, R. G. *Russ. J. Inorg. Chem. 9* (1964) 1177.
13. Olson, D. S., Kibler Jr., F. C., Seegmiller, D. W., Fannin Jr., A. A. and King, L. A. *J. Chem. Eng. Data 19* (1974) 27.
14. Berg, R. W. and Østvold, T. *Acta Chem. Scand., Ser. A 40* (1986) 445.
15. Werner, P.-E. *Z. f. Krist. 120* (1964) 375 and *Arkiv Kemi 31* (1969) 513.
16. Werner, P.-E., Eriksson, L. and Westdahl, M. *J. Appl. Crystallogr. 18* (1985) 367.
17. de Wolff, P. M. *J. Appl. Crystallogr. 1* (1968) 108.
18. Smith, G. S. and Snyder, R. L. *J. Appl. Crystallogr. 12* (1979) 60.
19. Rietveld, H. M. *Acta Crystallogr. 2* (1969) 65.
20. Wiles, D. B. and Young, R. A. *J. Appl. Crystallogr. 14*(1981) 149.
21. Young, R. A., Ed. *The Rietveld Method*, International Union of Crystallography, Oxford 1995.
22. Young, R. A., Sakthivel, A., Moss, T. S. and Paiva-Santos, C. O. *Program DBWS 9411, Rietveld Analysis of X-Ray and Neutron Powder Diffraction Patterns*, Georgia Institute of Technology, Atlanta 1994.
23. Staffel, T. and Meyer, G. *Z. Anorg. Allgem. Chem. 585* (1990) 38.

24. Rytter, E., Rytter, B. E. D., Øye, H. A. and Krogh-Moe, J. *Acta Crystallogr., Sect. B 29* (1973) 1541.
25. Rytter, E., Rytter, B.E.D., Øye, H. A. and Krogh-Moe, J. *Acta Crystallogr., Sect. B 31* (1975) 2177.
26. Troyanov, S. I. and Rybakov, V. B. *Organomet. Chem. USSR, 1* (1988) 700, Russ. p. 1282.
27. Troyanov, S. I., Rybakov, V. B., and Ionov, V. M. *Russ. J. Inorg. Chem. 35* (1990) 494, Russ. p. 882.
28. Shannon, R.D. *Acta Crystallogr., Ser. A32* (1976) 751.

Received June 14, 1996.